A STUDY OF HALL-EFFECT MEASUREMENT TECHNIQUES ON PULSED LASER ANNEALED GALLIUM ARSENIDE

by

TIMOTHY W. H. CHIN

B.S, Kansas State University, 1985

A MASTER'S THESIS

submitted in partial fulfillment of the

requirements for the degree

MASTER OF SCIENCE

Department of Electrical and Computer Engineering

KANSAS STATE UNIVERSITY
Manhattan, Kansas

1988

Approved by:

Andrzej Rys

Major Professor

TABLE OF CONTENTS

LIST OF FIGURES

ACKNOWLEDGEMENTS

I would like to thank the following professors and graduate students whom I have worked closely with in the course of this project. Especially to my major professor, Dr. Andrzej Rys, for his patience and guidance during the writing of this thesis.

Many thanks to Dr. Alvin Compaan and his graduate student, Ajit Bhat, for their advise and ideas throughout this project.

I would also like to thank Dr. Gale Simons and Dr. Anil Pahwa for serving on my commitee.

The ion-implanted GaAs samples donated by Mr. Ian Burrows of Honeywell Incorporated and Wright Patterson Air-Force Base, Dayton, Ohio is gratefully acknowledged.

Most of all, I would like to express my thanks to my "pals" who have supported me all these semesters.

* This thesis is supported in part by the National Science Foundation Grant(NSF) No. ECS-8505161 and by the NSF equipment grant No. CHE 8310646.

INTRODUCTION

1.0

It would perhaps be unfair to consider this section as an introduction to this thesis as it would be more appropiate to regard this as a continuation of the work left over by my predecessors. The study of Pulsed Laser Annealing in ion-implanted GaAs is by no means new to semiconductor processing. Research work for GaAs began at about the same time as work on silicon technology. The continued zeal on GaAs however was short lived due to a number of technology related problems in the past, hence setting silicon technology at the forefront.

In recent years, the demand for high speed digital integrated circuits have resurrected the interest in the field of GaAs semiconductor processing. Due to the high electron mobility and high peak electron velocity characteristic of GaAs, its substrate have been used in the development of fast switching high electron mobility transistors (HEMT). Thus, with the availabilty of more advanced processing equipment, extensive research have gone into developing viable processsing techniques for GaAs. Technically, the same fabrication techniques for silicon could be adapted for GaAs. Attempts in using traditional furnace annealing for GaAs, however, have been futile. Hence an alternative form of annealing is required.

The work on Pulsed Laser Annealing at Kansas State University began as a joint effort between Dr. Andrzej Rys of The EECE department and Dr. Alvin Compaan of the Department of Physics. With the assistance of their Graduate students Messrs. Arkady Horak, Huade Yao, and Ajit Bhat, a Pulse Laser Annealing set-up for an EXCIMER laser system was designed for research purposes. Unfortunately, major problems both attributed to the inability to obtain a homogenised laser beam as well as hardware flaws ,had prevented further studies on the effectiveness of PLA on ion-implanted GaAs.

My contribution towards the project soon led to continuation of the work initially spear headed by Mr. A. Horak. With the inexhaustible help of Mr. Ajit Bhat, we were able to re-develop a system which had enabled me to analyse the viability of PLA on GaAs substrates.

The scope of this thesis will primarily cover the study of carrier activation and mobility of pulsed laser annealed GaAs substrates. It will also discuss the effects of laser annealing on low dosed as well as heavilly dosed substrates. As the samples used in the experiments are silicon nitride encoated, the effect of encapsulant on the carrier activity will also be addressed.

The format of this thesis will essentially be based in the following fashion. Section 1.0 will cover briefly the

stoichemistry of GaAs and Si, and hence discuss the problems GaAs substrates encounter when subjected to the same processing techniques used for Si. Thereafter Section 2.0 will discuss the instrumentation and theory utilised in the course of the experiments. Section 3.0 and 4.0, will be devoted entirely to the results and conclusions drawn from the efforts of the project. All Hall-Effect data acquired for the inferences and plots throughout the thesis is included in the appendices.

1.1 Structural differences in silicon (Si) and gallium arsenide (GaAs).

Si is an element semiconductor that lies in Group IV of the Periodic Table of elements. Although silicon technology currently dominates in the semiconductor industry, it lacks various properties GaAs possesses. Perhaps the only similarity between the two semiconductors is the diamond shaped structure in which they are both arranged. GaAs, however is a compound semiconductor, where gallium (Ga) is a member of the Group III elements while arsenic lies in Group V of the periodic table. This unique crystal orientation, gives rise to certain electrical and optical properties that are absent in Si. For this reason, GaAs substrates are particularly favorable for the fabrication of microwave and photonic devices.

Earlier on we mentioned that both Si and GaAs possesses diamond structures. On close observation of the crystal lattice of Si on figure 1[a], one will notice that the structure is composed of two interpenetrating Face Centre Cubic (FCC) sublattices. The sublattices are displaced 1/4 of the distance away from the major diagonal with each corner and face occupied by a single silicon ion. In the case GaAs, the gallium atoms occupy one sublattice while the arsenic atoms occupy the other as shown in figure 1[b]. This crystal orientation is otherwise known as the Zincblende

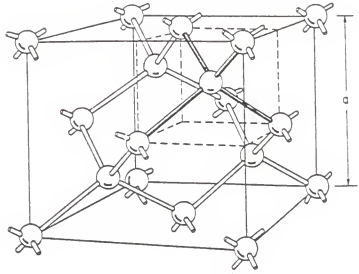

Figure 1[a] Diamond lattice structure of Si

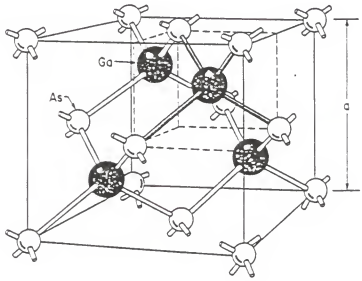

Figure. 1[b] Zincblende lattice structure of GaAs

lattice structure.

The electrical and optical properties of both Si and GaAs are best represented by their respective energy band diagrams. As mentioned previously, GaAs has a major advantage over Si in that it has inherent optical properties which Si does not possess. Consider the following band diagrams on figure 1[c] and 1[d].

The two most salient points between the two semiconductors are :

(A) Difference in Energy gaps (E_g). At room temperature, E_g(Si) is 1.12eV while E_g(GaAs) is 1.42eV.

(B) Difference in Crystal Momentum P.

Note that these two factors play a crucial part in the electrical activity of the two semiconductor. Consider the kinetic energy of a free electron in the conduction band of a semiconductor denoted by the following equation.

$$E = P^2/2M_n$$

where P = Crystal Momentum
M_n= Effective electron mass.

One will notice the strong dependency of the kinetic energy on the crystal momentum of the semiconductor itself. Thus for an electron to make a transition from the valence band to the conduction band, it will first have to overcome the energy gap E_g. For this occur, this requires a change in the Crystal Momentum P.

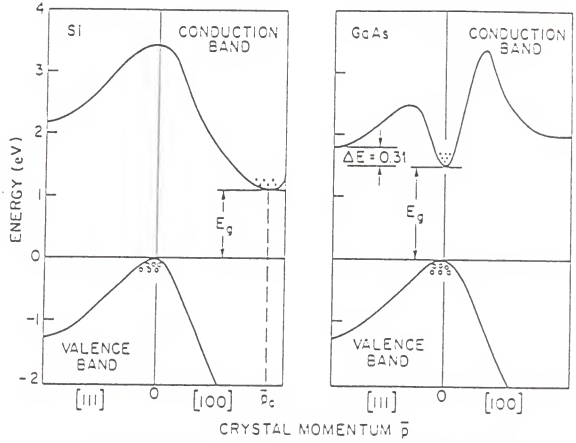

Figure 1[c]

Figure 1[d]

Energy band diagrams of Si and GaAs illustrating the direct and indirect nature of its properties.

In the case of silicon, from the energy band diagram of figure 1[c], the maxima of the valence band is displaced from the minima of the conduction band by P_c. Hence for conduction to occur, the two maxima and minima has to be aligned. This, therefore makes silicon an indirect semiconductor since it needs to undergo a change in crystal momentum.

GaAs, despite having a larger energy gap does not require any change in P as both the maxima and minima of the valence and conduction band occurs at the same crystal momentum P =0 (See figure 1[d]). Hence making GaAs a direct semiconductor. The nature of direct and indirect semiconductors is very important in the fabrication of photonic devices (light sensitive devices). GaAs, having the direct qualities , have often been the choice for optically active devices over silicon.

GaAs have often been touted as a semiconductor that promises high electron mobility. The effective mass of an electron M_n, follows a parabolic relationship denoted by the following equation:

$$M_n=[d^2E/dP^2]^{-1}$$

Since the energy-crystal momentum relationship is parabolic, the smaller the effective mass the faster the electron will conduct in the presence of a magnetic field. Since GaAs has a narrower conduction band parabola than Si,

it has a higher electron mobility. The combination of the direct nature and the enhanced electron mobilities of GaAs makes it particularly favorable for High Speed Integrated Circuit fabrication.

1.2 Advantages and Disadvantages of GaAs over Si

The advantages of GaAs on the whole outweighs those of Si when the two are compared. Structurally, GaAs although predominately bonded by covalent bonds between its Ga^+ and As^- ions, it possesses a weak ionic bond between them. Unlike Si, whose major bonds are covalent, GaAs having a weak ionic bond is more electrically active hence contributing to higher electron mobility. Other attributes of GaAs include, as mentioned previously, the direct nature of its crystal momentum which enables the semiconductor to be better suited for photonic devices. In addition, GaAs is not only tolerant of wide temperature changes (-200^oC to 200^oc) but is also resistive to radiation[2].

However, the one major factor that impedes the role of GaAs as the new substrate for commercial use is perhaps its cost. The price of GaAs wafers is nearly four times as much as silicon. Furthermore, the processing cost for such a sensitive semiconductor is currently too high for investors to risk upon. Note that GaAs has the disadvantage of exhibiting a larger density of damage than Si. The

probability of dislocations nearly doubles, taking into account the damage found in the gallium sites as well as those in the arsenic sites. Hence disrupting the electrical properties of the substrate.

These damaged sites can be "cured" using an annealing process and thus restore the substrate to its electrically active state. Several conventional annealing techniques as well as those in current research areas will be discussed in Section [1.4].

1.3 Purpose of Annealing

Two major methods of commercial doping for both Si and GaAs wafers are Furnace Diffusion and Ion-implantation. Both process are used to selectively dope semiconductor wafers to either n-type or p-type substrates. The former being a thermal process has the dopant material placed on or near the surface of the wafer whereby it is diffused into the subtrate at high temperatures. One will notice that the profile of the dopant concentration for the furnace diffusion decreases monotically from the surface as shown in figure 1.3[a].

Ion-implantation, however, has a more dependable and consistent profile. This low-temperature process involves the dopant ions being accelerated into the substrate by means of a high energy ion beam. This results in a peak in the dopant profile taking the form of a Gaussian

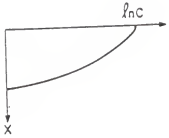

Figure 1.3[a] Profile of dopant concentration of a furnace diffused semiconductor sample as measured from surface along the distance X

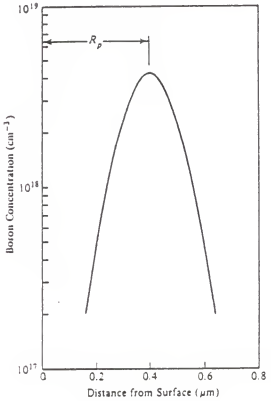

Figure 1.3[b] Profile of concentration of an ion-implanted semiconductor sample

distribution. (See figure 1.3[b]). Hence an approximation of the projected range of the implanted dopants can be easily varied by merely changing the ion beam energy.

For this reason, ion-implantation provides a more precise and controlled form of doping in comparison to furnace diffusion. The majority of the samples used in this thesis were obtained from various commercial sources. All were ion-implanted with n-type dopants on semi-insulating GaAs. P-typed implanted substrates will not be discussed although the annealing techniques in this research are easily applicable to p-typed GaAs. Typical donor impurities for GaAs include tellurium (Te) and selenium (Se) from Group VI of the Periodic table and Si from Group IV.

Ion-implantation may seem to be an effective form of controlled doping but it has its share of disadvantages. When an ion is accelerated into a substrate, it undergoes a series of electronic collisions before it comes to rest. This effect in turns leaves a tree of point defects along the way as shown in figure 1.3[c]. The continual bombardment of ions onto the crystal lattice of GaAs will then cause the inherent Ga and As atoms to be displaced from their respective sub-lattices causing the structure to become amorphous. This form of damaged is otherwise termed as Implantation induced damage. The amount of damage incurred is heavily dependent on the mass of the implanted ion. For

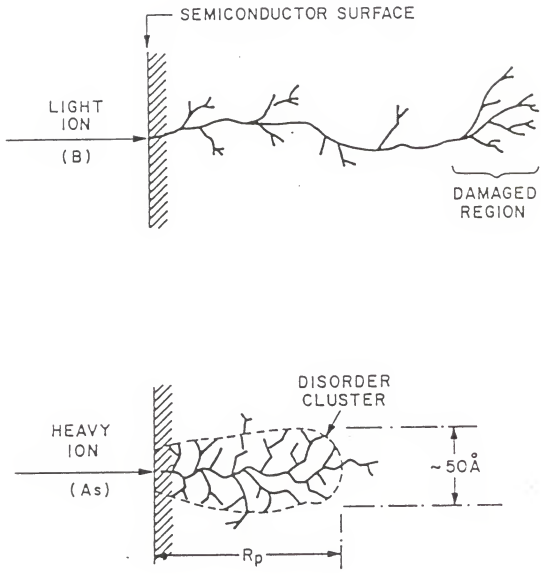

Figure 1.3[c] The effects of ion-implantation induced damage of both light and heavy ions, boron and arsenic.

instance, a heavier ion will result in a shorter penetration depth with a larger density of disorders while a lighter ion will go further into the substrate with a smaller density of point defects. In the case of n-type dopants implanted in GaAs, there are almost all heavy ions thus requiring high acceleration energy. Hence the probability of implant induced damage for these substrates is even higher.

Electrical characteristics, such as electron mobility and carrier lifetimes of ion-implanted GaAs, are severely degraded by the process of ion-implantation alone. For this reason the process of annealing becomes necessary to restore the activation of the implanted ions. A short definition for annealing is best described as a process which involves the rapid melting of the substrate surface layer and recovery of its displaced atoms to its previous subtitutional site. This can also be described as an epitaxial regrowth process hence re-activating the implanted donors.

1.4 Techniques of Annealing

Several techniques have been used commercially in semiconductor processing. To illustrate the pros and cons of these techniques, two main classes of annealing processes will be considered.

Local Process	Spot Process
Furnace Anneal (FA)	e-beam Anneal

Rapid Thermal Anneal(RTA) cw Laser Anneal

Pulsed Laser Anneal (PLA)

Furnace Annealing(FA) is a local process in that the substrate is "baked" to elevated temperatures in the range of 800 to 1000°C for approximately 30 minutes. Although the process results in 50 to 90% recovery of implanted ions, the carrier lifetime is diminished due to the build up of dislocation loops at such elevated temperatures. As carrier lifetime decreases, the mobility of the carriers tend to fall. Both the carrier activation and mobility of an annealed sample can be characterized experimentally using Hall Effect measurement techniques.

Although FA is currently the conventional process for Si technology, its applications towards GaAs are not as favorable. FA, primarily has little control over the uniformity of the annealed area of the substrate. Secondly, due to the high annealing temperatures, the two host species of Ga and As are especially sensitive to such temperatures. Hence, there is a considerable amount of outdiffusion of arsenic as it melts at 600°C.

From this, it is apparent that an alternative annealing technique is required for GaAs ion-implanted substrates. A great deal of research have gone into Rapid Thermal Annealing. Those methods classified under spot process are

some to name a few. In comparison to the traditional methods of FA, the annealing times for such processes are significantly faster. Pulsed Laser Annealing (PLA), is of particular interest. The technique is not entirely new as previous work using CW-lasers (Continuous Wave lasers) have been used to anneal ion-implanted Si substrates. Such a method would seem ideal for GaAs as it enables spot annealing to be done over a small area while allowing the rest of the substrate to remain at room temperature. However, the problem CW-lasers is faced with is its inability to provide a good uniform beam for PLA because of its low pumping rate. This problem was later rectified with the advent of the Excimer Halide gas filled laser.

1.5 Pulsed Laser Annealing (PLA)

The application of laser technology to semiconductor processing is not new. Extensive research have been conducted on the development of lasers towards the process of annealing. In Shunji Nojima's[1] paper on "Laser annealing effects in ion-implanted GaAs", he demonstrated the use of a Q-switch Pulsed Ruby Laser on Si implanted GaAs. From his observations, he found that the effective pulse laser annealing was dose dependent i.e , he found little to no sheet carrier concentration at low-dosed ion-implanted GaAs ($< 10^{14}cm^{-1}$). Secondly, he added that a variety of problems associated with the Solid State Lasers themselves had

restricted the scope of his experiments. The majority of the problems were solely due to the lack of sophistication in the hardware used. He found that the spatial homogeneity of the annealed region was generally poor and marred due to the laser's inability to provide a high pulse repetition rate. In short, the experiments conducted had utilised 1981 technology.

It wasn't until 1983 when the development of rare Gas Halide induced lasers were introduced for commercial use when further endeavours in PLA continued. Questek Lasers produced their line of EXCIMER lasers where the active medium for the laser was XeCl (λ=0.308μm), Xe and Cl being halogens. Unlike the Ruby laser (λ=0.694μm) that was previously used for PLA where its spectrum correspond to the deep red wavelength, EXCIMER lasers correspond to the Ultra-Violet region[5]. Thus, the penetration depth for EXCIMER laser is shallower than that of Ruby Lasers hence reducing surface damage.

Despite the promise of a halide laser with the ability to provide excellent beam quality and high pulsed repetition rates, a great deal of work had to be done to improve the beam quality to the standards required by laser annealing. To improve beam uniformity or homogeneity, additional optics was required. Much of the work devoted to the laser annealing process was conducted in the Laser Laboratory of

Ward Hall at Kansas State University. A Questek (Series 2000) EXCIMER laser was used to generate the high intensity beam. In attempting to homogenise the beam during the early stages of the project, it was found that there was a distinct trade off between the beam homogeneity and the power density across the annealed area. Thus, a larger beam spot area would result in the degradation of the laser power density. We were able to successfully produce a range of power densities from $0.2J/cm^2$ to $0.4\ J/cm^2$ across a beam spot no bigger than 3mm in diameter with a uniform beam homogeneity and power density.

To illustrate the necessity of a uniform beam, two annealed GaAs clover leaf spots are shown in figure 1.5[a] and 1.5[b]. Figure 1.5[a] shows an annealed region without its laser anneal beam homogenised while figure 1.5[b] shows the another sample annealed at the same energy with a beam homogenizer. Notice on figure 1.5[a] the "speckle" effect on the annealed surface. This irregularity shows that certain areas of the sample have been annealed with a higher laser intensity than others, thus leading to surface damage and low carrier activation. Figure 1.5[b] having been annealed across a beam homogenizer, shows a relatively smooth surface indicating that uniform annealing was performed throughout the sample. The orientation of the homogenizer along with the rest of the optical instrumentation will be discussed in

the next section in detail.

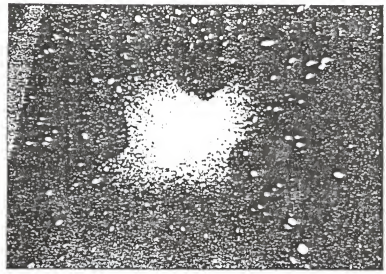

Figure 1.5[a] Magnified region of pulsed laser annealed GaAs sample in the absense of a beam homog eniser (X10). Sample measures 3mm by 2mm in dimensions

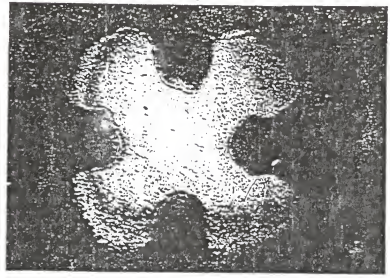

Figure 1.5[b] Magnified region of pulsed laser annealed GaAs sample with annealing beam homogenised (X10)

2.0 A descriptive overview of the Laser and Optical Instrumentation for PLA

With reference to figure 2.0a overleaf, the block diagram of the Laser system along with its optical set up for pulsed laser annealing is shown. Figure 2.0b, however, outlines the detailed orientation of the optics for the PLA system used in this project. Note that the distances and respective positions of the focussing lenses have been recorded to optimise both the uniformity as well as the pulse laser intensity of the beam.

Earlier on, it was mentioned that the largest beam spot achieved by the set-up was no larger than 3mm in diameter. One should note that the dimensions quoted on figure 2.0b have been arranged for a rectagular beam spot of 3 by 2 mm in dimensions. Should a larger spot be required, the orientation of the lenses would have to be altered with the possible sacrifice of an attenuated laser intensity across the anneal area.

With the exception of the beam intensity filter rack, the focussing lenses are mounted on a beam slide to ensure easy manoeuvre and optical allignment with the incident ultra violet beam. This rack contains slots for light filters to provide a range of power intensities. Each filter allows only 90% transmission of the incident beam. Since the

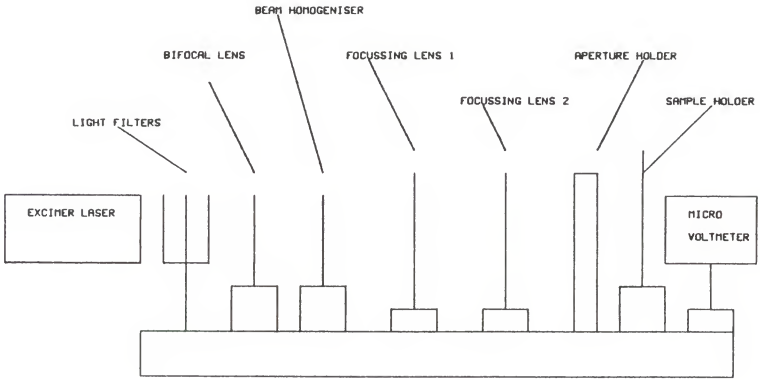

Figure 2.0[a] Block diagram of Pulsed Laser Annealing (PLA) System.

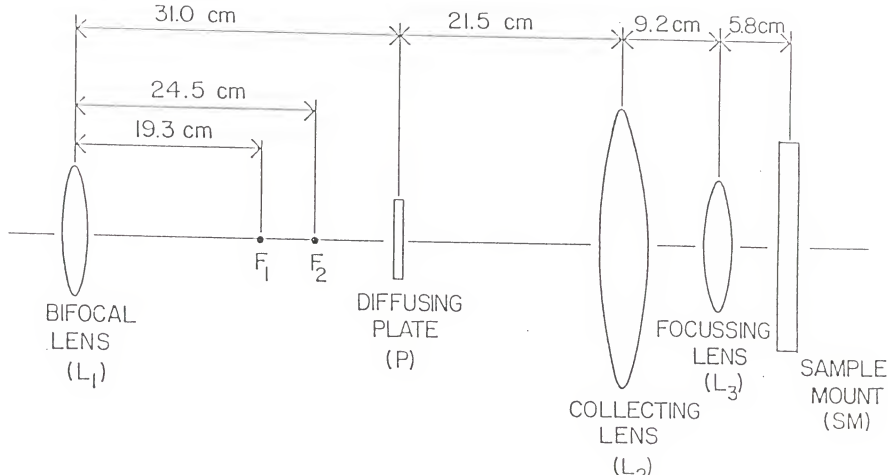

Figure 2.0[b] Optics set-up for PLA system

filters are not focussing in nature, they merely require allignment with beam. Starting from the right of the EXCIMER laser aperture, the following lenses and their applications are as follows:

[1] **Bifocal Lens (L1)** Almost self explanatory, the lens has two focal points with f1 at 19.3cm and f2 at 24.5cm. The purpose of this lens is to "squeeze" the incoming rectangular beam into a square. The lens is placed directly in front of the Filter rack.

[2] **Diffuser Plate (Beam Homogeniser)** This apparatus is perhaps the most crucial item in the set up. It is placed 31.0cm away from the Bifocal lens and provides a collimated light source. The plate, with both sides roughened, acts as a multiple point source. With each point on the plate as an independent light source, the incident beam when focussed will be homogenised.

[3] **Collecting Lens(L2)** Placed 21.5cm away from the Diffusing Plate, this lens is the first of the two focussing lenses to obtain an optimum beam spot of 3mm in diameter for PLA.

[4] **Focus Lens (L3)** Second focussing lens placed

9.2cm from L2.

[5] **Aperture Holder** The holder is placed 5.8cm behind the second focus lens (L3). This is to ensure that the focussed incoming beam provides an area to cover the aperture region. The aperture itself is essentially a mask to prevent the regions beyond the aperture size from being annealed. In the case of this set-up, a 3 by 2 mm rectangular pattern was cut off from a thin strip of metal by means of a Nd:YAG laser. A Clover Leaf pattern was later used for actual Pulsed Laser Annealing.

[6] **Sample Holder** The sample holder is attached onto a Two-Axis Stepper Motor (Maxwell Electronic Inc.) to enable continous spot laser annealing i.e raster scan across the wafer. (See Horak[8]). The Stepper Motors are computer controlled via a HPIB /IEEE 488 bus by a HP-86 computer. All programs controlling the movements of the holder were written in HP-Basic. For special programming commands regarding the Stepper Motors, see manuals. Note that the Sample Holder is placed as close as possible to the Aperture holder. The reason for this is to ensure laser annealing across the aperture onto the mounted sample.

To ensure perfect beam homogenity, a

thorough check of the beam profile should be undertaken prior to laser annealing. Thus, a profile of the beam across a circular aperture of 200μm in diameter was conducted. The profiles plots for energy intensity against the horizontal distance across the 3mm spot are included in appendix IV. From these plots, one will notice a relatively flat plateau of uniform laser intensity. The "speckle" effect caused earlier in a non-homogenised laser system was attributed to the fact that the profile across the aperture was composed of spurious peaks instead of the continous plateau now attained. The profile however does not guarantee a uniform beam at all times as the power intensity of the beam is dependant on the gas lifetimes of the active medium used.(in this case XeCl) Thus, the following procedures should be carried before laser annealing:

[A] Check gas pressure of active medium. (Reference to Questek Manual)

[B] Ensure beam slide is perfectly alligned with incident laser beam.

[C] For a "quick and dirty" check of the beam uniformity across the aperture, place a strip of fast exposing photographic paper close to the aperture. Reduce the intensity of the incoming beam using the light filters to prevent over-exposure of the paper. Take single shots of the beam and examine the uniformity of exposed area.

[D] To check the power intensity of the beam spot. All light filters should first be removed. On doing this, measure the equivalent voltage transmitted across the 3 by 2mm aperture using a Calorimeter. In this system, a Kiethley 155 Null De-

tector Microvoltmeter was used. Thereafter set the Repetition rate of the laser at 5 pulses/sec at and an energy of 100mJ. Using the following conversion, calculate the maximum laser intensity for the system:

For a 3 by 2 mm aperture:

1mV ---------- 0.069 Jcm^{-2}.
(Refer to appendix IV for details)

Since the ion-implanted sample is to be annealed across the aperture mask, it is imperative to keep the semiconductor free from dust particles and ,in particular, fingerprints. GaAs or Si wafers, in the first place, should not be handled with bare hands. Therefore, tweezers should be used at all times. As the majority of the samples are encapsulated to prevent surface outdiffusion of of arsenic, fingerprints can cause scratches to occur on the surface thus damaging the caps. These encapsulants will be discussed further in detail.

When cleaning the samples, solvents are best avoided as certain caps have adverse effects towards these chemicals and may be etched off inadvertently. The safest method of wet cleaning is by submerging the sample in deionised water for 3 minutes and blow dry it using a nitrogen gas gun.

Having done this, the sample is ready to be mounted onto the sample holder for laser annealing. Paraseal wax or Rubber cement is suggested for adhesive purposes. Wax, however, is ideal for sample mounting as it can be easily removed at low temperatures without causing damage to the

sample.

2.1 The Hall Effect Theory

The Hall Effect technique is widely used in determining the electrical characteristics of active semiconductor substrates. It is by far the most effective method of quantifying the degree of free carrier activation as well as its carrier type. Hence this method is applicable to both n-type and p-type semiconductors.

To develop the theory behind this technique, consider the follwing n-typed semiconductor bar, whose majority carriers are electrons.(See figure 2.1[a])

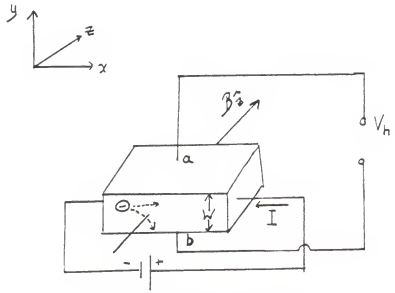

Figure 2.1[a] The Hall effect

When a magnetic field, Bz, is applied at right angles to the direction of the current flow, Vx, across the bar, the electrically active n-typed majority carriers are

subjected to a Lorentz Force Fl. The downward motion of the electrons is attributed by magnetic field Bz being balanced by the electric field, qEy. This phoenomena is otherwise called the Hall-Effect. To illustrate this, the following equations are denoted:

$$Fl = q(Vx \times Bz) \quad \text{..... (eqn1)}$$

where, q = Charge of an electron
Vx = Electron drift velocity
Bz = Magnetic field

By equating the Magnetic field to Electric field:

$$(-)qEy = q(Vx \times Bz) \quad \text{..... (eqn2)}$$

The Electron drift velocity, Vx, can be re-expressed in terms of the Current Density Jn and the Hall Coefficient, Rh. By simple mathematical manipulations, a relationship for the carrier concentration can then be developed.

Hence,

$$(-)Ey = RhJnBz \quad \text{..... (eqn3)}$$

where,
Rh = (-)1/qn for n-type carriers.
= or 1/qp for p_type carriers.
Jn = Current density
n = n-type carrier concerntration.

By substituting Rh into eqn3 :

$$(-)Ey = (-)JnBz/qn$$

$$n = JnBz/qEy$$

Since Jn = I/Area and Ey = Vh/W where Vh(Hall Voltage) is the potential difference measured across W, the

thickness of the bar from a to b.

Thus,

$$n = (I/Area)Bz/q(Vh/W)$$

$$n = IBzW/qVhArea \ldots\ldots \text{eqn4}$$

Since the thickness of the sample is not known and assuming the sample to be symetric of dimension d, the sheet carrier concentration can be determined instead. Thus, by manipulating the equation, the following expression for sheet carrier concentration is obtained.

$$n.d = BzI/\ Vhq \quad [m^{-2}] \ldots\ldots \text{eqn5}$$

By measuring the Hall Voltage Vh across a and b, at a fixed magnetic field with a constant current source I, the type and concentration of activated carriers can easily be calculated. Note that all Hall Data collected in this thesis is in units of cm^{-2}.

Electron mobility, u_n, is inversely related to the sheet resistivity, ρ, and sheet carrier concentration, n.d, of the semiconductor sample. With the latter found previously using the Hall measurements, the sheet resistivity, ρ/d, remains to be the only parameter to be measured. Thus, it is suggested that the two measurements be conducted in parallel. The following equation should first be considered:

$$\sigma\text{(Conductivity)} = 1/\rho = q(nu_n + nu_p) \ldots\ldots \text{eqn6}$$

Since the conductivity of the holes and electrons are additive, the following assumption can be made:

$$\sigma = 1/\rho = qnu_n \quad \text{for n-type carriers}$$

Hence,

$$u_n = 1/qn\rho \ldots\ldots \text{eqn7}$$

where, u = Electron Mobility
n = Carrier Concentration
ρ = Resistivity
q = Charge of an electron.

There are essentially two common methods in measuring sheet resistivity, namely the 4-point technique and L.J Van Der Pauw[1] method[10]. The 4-point probe [13] despite being the most common method used for measuring the resistivity of semiconductor wafers, is unsuitable for the pulsed laser annealed samples. The reason for this is simply because the distances between the probes (6 mm) exceed the 3 mm region of the annealed diameter. Since the 4-point probe requires all four test points to be in close contact of the annealed sample, this method was rejected in favour of the Van Der Pauw technique.

The Van Der Pauw technique has the advantage of being applicable to flat semiconductor samples of arbitrary shape. Consider the following sample cut out as a flat lamellae of an undefined shape.(See Figure 2.1[b])

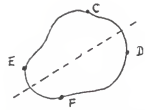

Figure 2.1[b] Van der Pauw sample of undefined shape

By choosing four points C,D,E, and F on the periphery of this lamellae, the sheet resistivity of the sample is related to the following equation:

$$\exp(-\pi d R_{CE,FD}/\rho) + \exp(-\pi d R_{EF,CD}/\rho) = 1 \quad \text{.....eqn8}$$

where, d = Thickness of lamellae
$R_{CE,FD}$ = Average resistance of CE,FD
$R_{EF,CD}$ = Average resistance of EF,CD

To elaborate further, this method merely estimates the resistivity by determining the average resistance between the two positions EFCD, and CEDF of the lamellae. How does this come about? These two resistances are determined in the following manner. $R_{CD,EF}$ is found by applying a constant current, i, across the positions EF and measuring the potential difference developed across the positions CD.

$$R_{CD,EF} = (Vc-Vd)/ief$$

$R_{EF,CD}$, can be determined in a similar fashion. Notice that the objective of this method is to calculate the average resistance of the sample as can be shown in a general equation of the Van Der Pauw lamellae below.

$$\rho = d(R_{CE,FD} + R_{EF,CD})f/2\ln 2 \quad \text{.....eqn9}$$

where, f= Correction Factor = $R_{EF,CD} / R_{CE,DF}$

Once again, the resistivity of the lammalae will have to be expressed in terms of sheet resistivity to maintain the dimensions of sheet carrier concentration determined earlier. Thus, eqn9 can be rewritten as:

$$\rho/d = (R_{CE,FD} + R_{CF,ED})f/2\ln 2 \quad \text{.....eqn10}$$

The Correction Factor, f, is to compensate for the asymetricity of the sample. Should the lammelae be symetric in shape, in theory $R_{EF,ED}/R_{CE,FD}$ should equal to 1 which gives a Correction Factor of 1, as obtained from the graphical representation of the Correction Factor function. (See figure 2.1[c])

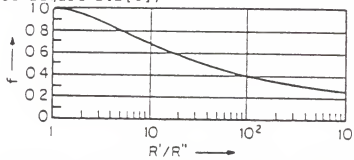

Figure 2.1[c] Correction factor chart

A thorough mathematical derivation for the Correction Factor function can be found in reference [10]. Now that the measurement techniques for characterising the electrical activity of an arbitrary shape semiconductor have been defined. The applications of the abovementioned techniques towards a Clover Pattern will be discussed in the following section.

2.2 The Van Der Pauw Clover Leaf Lammelae

The accuracy of Hall measurements is dependant upon the shape and size of the Hall sample. An ideal sample would be one with a symetrical shape. Should the sample be square, the Hall contacts (Indium was used on the GaAs test samples), are to be made infinitely small and placed on each corner of the sample. The reason for having such small contacts is to prevent any distortion of the current flow during the course of the measurements. At this point, one should also consider the effects of spurious potentials due to the asymetricity of a sample. Hence if one considers the flat symetric sample shown in figure 2.2[a] below, as current flows across C,F of the sample, equipotential lines will be found along position D and E. Thus, on measuring the potential difference across D,E in the absense of a magnetic field, Vde, should give a static reading of zero volts.

However, on the average most of the cleaved samples are asymetric in nature hence recording a significant static voltage which should be taken into account when calculating sheet carrier concerntration.

The problem of "stray potential differences" can be rectified by introducing "ears" to the sample. (See figure 2.2[b]).

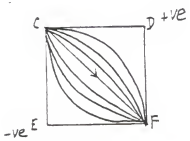

fig.2.2[a]

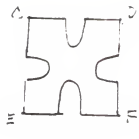

fig2[b].

By modifying the sample into a Clover Leaf Pattern as shown, the effect of spurious potentials and noise is reduced. This orientation would not only set the Hall contacts in symetry with each other but also prevent the contacts from shorting each other.

Due to the brittle nature of GaAs, it would be almost impossible to cleave such a pattern with small dimensions (3 mm from leaf to leaf) from the wafers. The alternative method would be to pulse laser anneal the ion-implanted wafer across a Clover Leaf mask in the same manner as decribed in section 2.0 . The pattern can be cut from a thin piece of sheet metal using a High Intensity laser beam . One such laser used in this project was the Nd:YAG (Quanta Ray DCR) Infrared Laser. A program to generate the Clover Leaf Pattern was written by A. Horak on a HP-86 computer. With the aid of an IEEE488 bus, the computer was interfaced to a computer controllable two-axis Stepper Motor where the sheet metal to be cut is mounted on an X-Y stage. The sheet metal is then moved along the orientation of the Clover Leaf

pattern and cut sequentially by the laser.

2.3 Instrumentation for Hall effect measurements

All Hall data acquired was conducted in the Magnetics laboratory in the Department of Physics at Kansas State University with the kind permission of Dr. George Hadjapanias. This section outlines the instrumentation used in performing the Hall readings, with reference to figure 2.3[a] overleaf.

[1] **Hall Probe** This is a specially constructed mount for the test sample. (See figure 2.3[b] for a closer view of the copper mount.)

[2] **Current Source Model 110, Lakeshore Cryotronics** Provides a constant current source for the Hall system. Since the samples are sensitive to temperature changes, small currents are used to avoid resistive heating which may cause erratic Hall potentials.

[3] **DVM 8520A FLUKE** Used to measure Hall potentials.

[4] **4-inch Electromagnet System V2300A, Varian Associates Instruments Division** Provides a maximum of 0.7Tesla(7KGauss) of constant magnetic field.

[5] **Gaussmeter 912, RFL Instruments, Booton Ltd.**

This instrument is equipped with a Gauss probe that measures magnetic field to within 0.4% of set reading.

On conducting the Hall effect measurements, one should perform the experiments away from any high frequency equipment as they contribute to spurious currents to the sample. In addition GaAs, being extremely sensitive to light, should have its static potential measured in the dark. An outline of the procedures taken to prepare the annealed samples is included in appendix II.

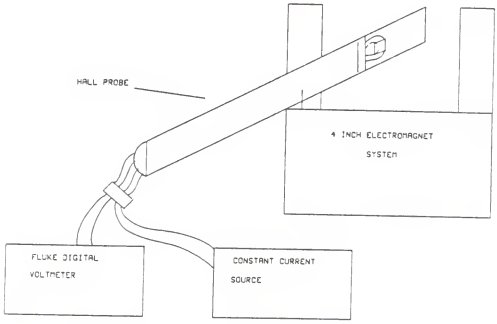

Figure 2.3[a] Hall effect set up.

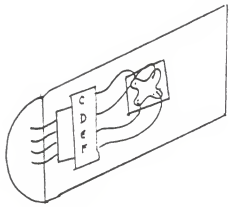

Figure 2.3[b] The Hall probe.

2.4 Effectiveness of Hall Effect measurement techniques

Two GaAs samples were subjected to the Hall measurements. One being cleaved from an n-type Telerium(Te) doped semi-insulating GaAs wafer and the other from a p-typed zinc doped substrate. The purpose of these prelimary readings is to demonstrate the validity of the technique when applied to substrates of different dopant types. Since the samples were obtained from separate commercial sources, the doping processes were invariably different. The Te doped sample was doped using a Vapour Phase Epitaxy (VPE) process. This process entails the dopants being grown into the substrate in its vapour form. The zinc doped sample is doped using a conventional Furnace Diffusion process. For a complete tabulation of the results and data for the two samples, refer to appendix I.

For the calculations obtained for the samples, one will notice the reliability and consistency of the Hall results. In the case of the Te doped sample, the average free sheet carrier concentration was 8x16 cm^{-2}. By estimating the wafer thickness to be approximately 0.05 cm, the activated carrier concentration of the sample would then be 1.6x18 cm^{-3} which is nearly 50% of the as evaporated dose of 3x18 cm^{-3}. Similarly, by the Van der Pauw technique, the Hall mobility of the sample was found to be 1848.9 $cm^2/V.sec$.

According to the impurity concentration/mobility plots for n-type GaAs in figure 2.4 below[11] , the electron mobility for a dose of $3x18cm^{-3}$ corresponded to a value of 2000 $cm^2/V.sec$ at 300K. From this one can justify the reliability and ease of the Hall technique in characterising electrical activity of doped substrates.

Once again, the effectiveness of the method can be applied to p-type substrates. The p-type concentration of the Zn doped sample was found to be $8.38x17cm^{-3}$. The measured hole mobility for this sample was approximately 149.01 $cm^2/V.sec$. Since the effective mass of holes is larger than that of electrons, the hole mobility for p-typed GaAs is measurably smaller than the n-typed substrates. From the mobilty plot of figure 2.4, the hole mobility value corresponding to the impurity concentration of $8.38x17\ cm^{-3}$ is 180 $cm^2/V.sec$ which is a good approximation of the measured hole mobility of 149.01 $cm^2/V.sec$.

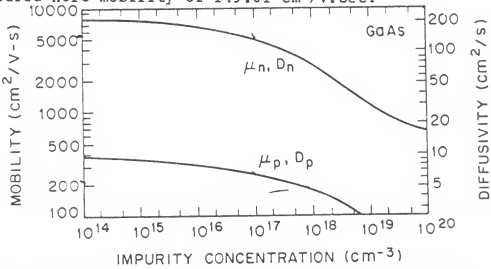

Figure 2.4 Mobilities and diffusivities in GaAs at 300K as a function of inpurity concentration.

Although the two abovementioned samples show promising results, both samples are highly doped (>> 1x16 cm^{-2} (1x18 cm^{-3}) involving a high temperature process. Impurity concentration, as will be seen later in section 3.0 plays a major role in the behaviour of the activity of the doped samples. The following section will deal with both Low dosed (<<1x14 cm^{-2}) as well as very heavily doped n-typed GaAs substrates. All of which have been pulsed laser annealed using a fast low-temperature process unlike the previous two samples mentioned.

DISCUSSION

3.0

This section will cover extensively the experiments and observations conducted on pulsed laser annealed GaAs substrates using an EXCIMER laser (λ=308nm) with a pulse duration of 10 nsec. The substrates used are semi-insulating and ion-implanted with n-typed impurities over a variety of doses ranging from low doses of 2.2x12 cm^{-2} to higher doses of 2x14 cm^{-2}. As mentioned earlier, the samples are all encapsulated with a layer of Si_3N_4 with a thickness of approximately 60nm. This is to prevent surface out-diffusion of arsenic during the process of annealing. Details on ion-implantation energies and cap thicknesses for the individual samples are included along with their respective Hall measurement results in appendix I.

Before continuing further into the analysis of the results, a short discussion on the importance of encapsulants should first be addressed. This discussion is of particular importance as the encapsulants play a vital role in limiting the laser power intensity for the purpose of laser annealing.

3.1 Encapsulants and their purpose

Although a variety of thin film encapsulants is available[4] for Group III to V semiconductors, Si_3N_4 is perhaps the most effective among those of Si, SiO_2 and AlN.

To demonstrate the effectiveness of the cap, two samples of Se implanted GaAs were prepared, one with its cap etched off, the other with its cap intact. Both of which were pulsed laser annealed at the same power intensity. Despite PLA being a spot process, the intensity of the laser is sufficient to cause a major degradation in electrical activity, even after a single pulse. From the Hall results of these samples, we found that while the encapsulated sample gave a high carrier activation, the other with the cap removed gave only 1% of its original implanted dose.

It has also been discovered [Compaan, Bhat et al][9], by direct Time resolved Transient Reflectivity of PLA Si_3N_4 encoated GaAs, that the melting threshold of the cap using an EXCIMER laser is 0.3 Jcm^{-2}. Thus, no annealing would have taken place below this threshold. On the other hand, should the laser intensity exceed the threshold to such an extent that the cap is blown off in its entirety, anneal damage will occur hence adding more damage to the substrate instead of "curing" it. The approach to this problem was to painstakingly pulse anneal the samples over a range of intensities and simultaneously test for its carrier activity until the optimum range for PLA is achieved. Thus, from the combination of the Hall results obtained along with the kind permission of Dr A.Compaan et al for the use of their Reflectivity results, we were then able to limit the laser

intensity from 0.17 to 0.4 Jcm^{-2}.

3.2 Analysis of ion-implanted pulsed laser annealed GaAs by the Hall Effect measurements.

Three ion-implanted doses were considered in the course of the research. They are as follows:

[i] Se/GaAs at 2.2x12 cm^{-2} (320 keV)
[ii] Si/GaAs at 6x13 cm^{-2} (140 keV)
[iii] Si/GaAs at 2x14 cm^{-2} (140 keV)

All data concluded from the measurements can be found in appendix II. A table consisting of the overall results for electron mobility and free sheet carrier concentration is shown overleaf in figure 3.2a.

It has been reported by Nojima et al, that the effects of PLA on low dosed Si/GaAs (<<1x14 cm^{-2}) show little to no carrier activation when a Q switch pulsed ruby laser was used. Our results, however, indicate the contrary. Consider sample (i), Se/GaAs at 2.2x12 cm^{-2} which is well below what is considered a low dose sample. We found the free carrier concentration to have exceeded the ion-implanted dose. These additional dopants could not have possibly materialised from nowhere thus it is to our conclusion that these dopants could only have originated from the Si_3N_4 cap itself. Using the Van Der Pauw technique, however, we found an alarmingly low electron mobility for the sample indicating the existence of residual damage. This, we believe, is possibly attributed to the additional dopants that were driven in

Hall Effect Results
All samples encapsulated with Si_3N_4
(Ion Implanted Dose = 2.2x12cm-2)

Sample Type	Laser I (Jcm-2)	n.d (cm-2)	Mobility (cm2/V-sec)
Se/GaAs (Capped)	0.27	2.604x12	116.65
Se/GaAs (Capped)	0.3	2.03x13	41.47
Se/GaAs (Capped)	0.33	1.48x13	69.07
(ion-implanted dose = 6x13 cm^{-2})			
Si/GaAs (Capped)	0.32	8.89x12	25.63
Si/GaAs (Capped)	0.29	7.84x12	92.6
Si/GaAs (Capped)	0.24	6.75x12	5.1
Si/GaAs (Capped)	0.23	1.02x12	56.1
(ion-implanted dose = 2x14 cm^{-2})			
Si/GaAs (Capped)	0.265	7.4x13	273.22
Si/GaAs (Capped)	0.24	3.64x13	234.01

Figure 3.2[a] Table of Hall effect results.

from the cap within. From this observation, the following conclusions can be drawn.

[A] That high carrier activation for low dosed ion-implanted GaAs can in fact be achieved by PLA, contrary to previously reported results.

[B] The nature of encapsulants is twofold. Although it reduces outdiffusion of arsenic from the substrate surface, it introduces additional n-type dopants from the Si ions from the cap during the process of laser annealing. As a result, it causes a certain degree of lattice damage which in turn causes the low electron mobility found. This can clearly be seen from the decreasing trend in electron mobility as the laser power intensity is increased from 0.27 to 0.33 Jcm^{-2}.

Sample (ii) and (iii), despite being laser annealed across an encapsulant, did not show any indication of additional doping as expected. These samples, however, were implanted at much higher doses of 6x13 cm^{-2} and 2x14 cm^{-2} respectively. Although the free sheet concentration measures below their implanted doses, one cannot rule out the possibility of impurity doping from the encapsulant. These results merely justify that the low dosed Se implanted GaAs substrate of sample (i) should be considered separately from

the higher dosed samples of (ii) and (iii). These two samples differ from the low dosed one in that a lower degree of activated implants was obtained than the former. Thus any additional doping from the caps would be insufficient to make any noticeable difference on the free sheet carrier concentration. With this in mind, it would be plausible to state that a dose dependency is observed for pulsed laser anealing. A possible explanation for this would be that EXCIMER lasers, having a shorter penetration depth (13nm for crystalline GaAs), is more applicable for shallow junction annealing for lower dosed samples.

From the composite plot of figure 3.2b, one will notice a trend similar in all three samples where the sheet carrier concentration steadily increases with laser intensity until it peaks at an optimum point between the range of 0.265 to 0.32 Jcm^{-2}. In both cases, however, the electron mobilities measured gave very low results. Figure 3.2c shows a plot for the corresponding electron mobilities for the three samples.

3.3 Other methods of characterising carrier activation

At this juncture, one should acknowledge the work conducted by Dr. A. Compaan et al on the Raman back-scattering studies of PLA ion-implanted GaAs. Using a light scattering technique as an alternative to the electrical measurements performed, Dr Compaan was able to characterise the degree of carrier activation of the substrates. Due to

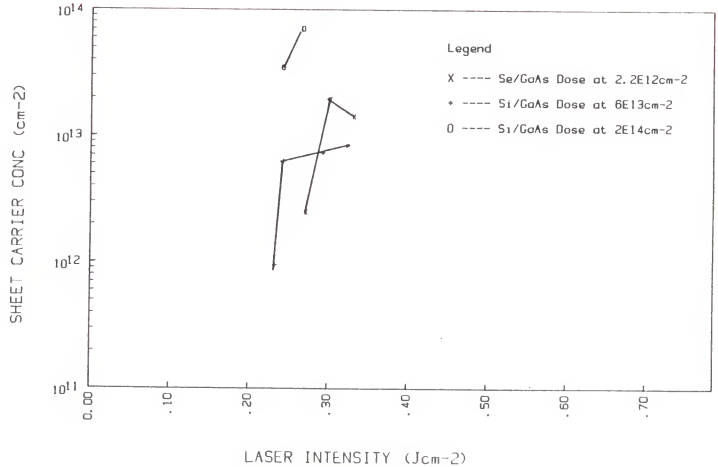

Figure 3.2[b] Hall effect measurements of carrier activation at various laser intens ities for ion-implanted GaAs substrates.

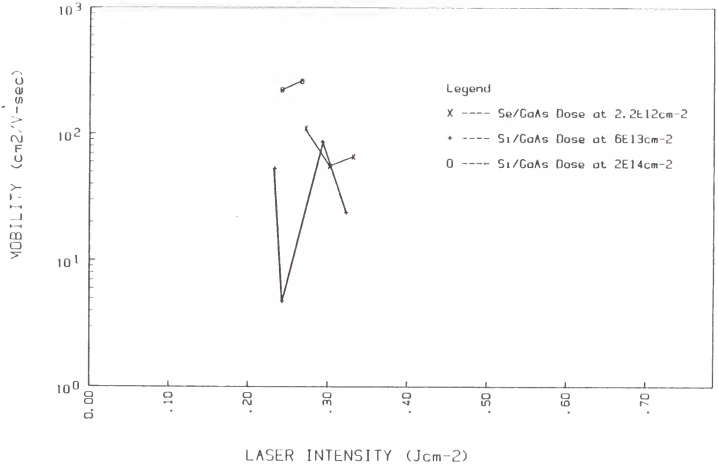

Figure 3.2[c] Hall effect measurements of carrier mobility at various laser intensities for ion-implanted GaAs substrates.

the complex nature of this topic, only a brief discussion of the method is addressed.

In brief, Raman spectroscopy involves the phenomena of a change in frequency of light when it is scattered by molecules. Thus, the frequency of an incident beam of monochromatic light spot focussed on an object will be subjected to a frequency shift. This frequency change then invokes an energy change that is characteristic of the irradiated object.

Two pulsed laser annealed samples that were previously analysed for carrier activation using the Hall method were sent to Dr. A. Compaan for further analysis using the back scattering technique. The two samples doses, 6x13 cm^{-2} and 2x14 cm^{-2}, both of which were found to be electrically active for the Hall measurements, were sent for further investigation.

A Raman study of the lower dosed sample at 2.2x12cm^{-2} was not possible as the sample was severely damaged soon after the Hall measurements were performed. However, for consistency another sample pulsed annealed at the same energy with an implanted dose of 6x12 cm^{-2} was analysed instead.

Shown in appendix III, are the Raman signals that were obtained for the samples mentioned that were annealed at various laser intensities. Notice that each Raman plot

posesses two distinct peaks. One, the normal Brilloun-zone centre (LO) characterises the carrier-free region on the surface whilst the other (L-) characterises the region with the density of active donors. Hence, the ratio of (L-/LO) is essentially a measure of the degree of carrier activation. Thus, the existence of a strong peak at (L-) would indicate a high degree of carrier activation at a particular spot on the sample.

To illustrate the composite result for the intensity ratio (L-/LO) for the samples, the plots on figure 3.3[a] and 3.3[b] shows the degree of carrier activation in terms of intensity ratio (L-/LO) against varying laser power intensities. Figure3.3[a] illustrates the two high dosed samples while figure 3.3[b] shows that of the lower dosed one. From the two plots,it can clearly be seen that there is a close association of the light scattering results to that of the electrical measurements made using the Hall technique. In particular, the higher dosed samples show a direct correlation between our results. The lower dosed sample, however, gave little sign of carrier activity from the Raman results contrary to our Hall results. This anomaly could be attributed to several reasons.

Primarily, the light scattering technique studies were carried out using a spot by spot analysis. In other words, only a small area of the annealed substrate is analysed each

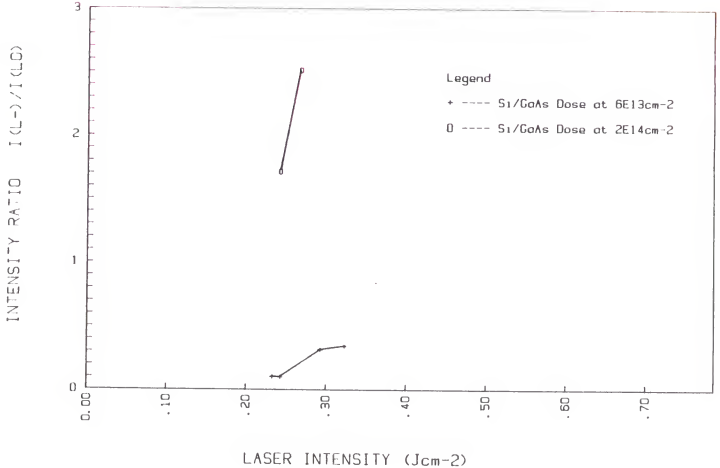

Figure 3.3[a] Intensity ratios for high dosed ion-implanted GaAs substrates by Raman back-scattering techniques.

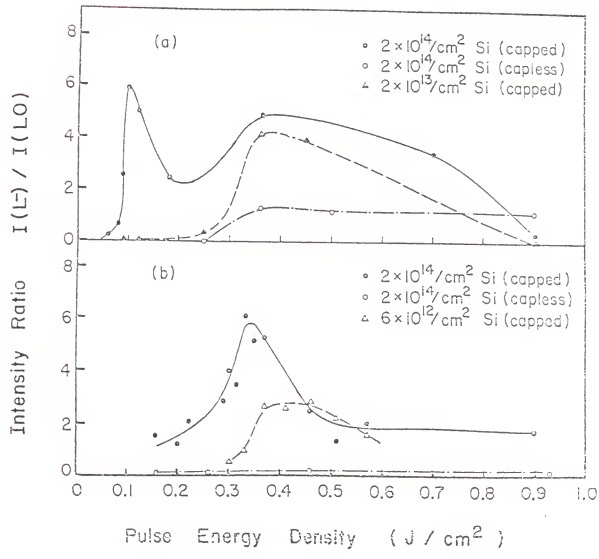

Figure 3.3[b] Intensity ratios for lower dosed ion-implanted GaAs substrates by Raman back scattering techniques.

time. The Hall effect measurement, however, provides an average reading of the sample since the whole clover-leaf sample is taken into account. Hence, the Hall effect technique is a more comprehensive method of characterising the free sheet carrier concentration for lower dosed samples. Secondly, the sample ($6x12\ cm^{-2}$) in question was not identical to the one that was previously analysed using the Hall method. Despite this, there is a clear indication that the laser intensity range from $0.265\ Jcm^{-2}$ to $0.32Jcm^{-2}$ was probably the best levels for laser annealing.

CONCLUSION

4.0 The process of pulsed laser annealing for ion-implanted GaAs by means of an UV Excimer laser (λ=0.308μm) is presented in this thesis. Having studied a variety of pulsed laser annealed samples ranging from $2.2x12cm^{-2}$ to $2x14cm^{-2}$, we can show by using conventional Hall Effect techniques that pulsed laser annealing can effectively remove implant damage for both low dosed as well as very heavily doped GaAs subtrates. To support this statement, the following conclusions were drawn pertaining to the PLA system set up at our laboratories.

Primarily, high carrier activation was observed at room temperature (300K) for low dosed Se implanted GaAs, contrary to earlier efforts using a pulsed ruby laser. The action of additional doping from the Si_3N_4 encapsulant during the anneal process was also noted hence attributing to carrier activation that exceeds 100%. This, however, was not so for the higher doped samples which only gave 37% recovery of its as implanted dose. Hence, a dose dependancy is observed, coinciding with experimental results of earlier reports [2]

Secondly, we find that despite sucessful attempts in carrier activation recovery, the overall electron mobilities for all three samples gave exceedingly low readings (<< 300 $cm^2/V.sec$). As mentioned in section 3.2, we do not know, at this point the actual cause for such low mobilities.

However, we have a strong indication that the problem may be attributed to the excess dopants introduced from the encapsulants during annealing. A comprehensive study of the deep level carrier traps present in the laser annealed samples may help determine the correlation between the low electron mobility readings and the defect traps. This may be carried out using a deep level transient spectroscopy technique(DLTS). DLTS involves a high frequency capacitive thermal scanning process where the defect traps of the samples can be characterise. Such experiments are currently underway.

The problem of low electron mobility is crucial to semiconductor device fabrication as the majority of fast switching field effect transistors and diodes require materials that are high in electron mobility (8500 $cm^2/V.sec$) as well as being lightly doped. Hence, it is essential that future work be conducted in this specific area.

Finally, a third observation can be drawn regarding the laser power intensity for effective annealing. Note however that the following values quoted pertain to the Excimer laser used under the conditions described in Section 2.0. We found the optimum laser intensity for annealing to range from $0.265Jcm^{-2}$ to $0.325Jcm^{-2}$. These results were supported by the Raman profiles for the samples and provided with the

kind permission of Dr. Alvin Compaan and Mr. Ajit Bhat of the Department of Physics, KSU.

To conclude, one may rather standoffishly state that the future of GaAs is limitless once perfected. However, this is entirely dependent on the type of processing technology used to perfect the substrates for device fabrication. With ultra violet rare halide gas lasers, we were able to provide an alternative annealing process with a modicum of favourable results. It is to our intentions that PLA might lead to a process that will completely eliminate the need for an ion_implantation step. Thus, being possible to implant as well as anneal the substrates at the same time.

Appendix I

Hall Effect Results

Sample Type : Te/GaAs Square sample
Impurity Concentration: 3el8 cm-3
Doping Process: VPE(Vapour Phase Epitaxy)
Vstatic: 0 Volts

==========

Magnetic Field = 1 Tesla

I(mA)	Vfor	Vrev
3	19uV	- 23uv
10	69uV	- 70uV
30	209uV	- 210uV
100	701uV	- 701uV

==========

Magnetic Field= 0.5 Tesla

I(mA)	Vfor	Vrev
3	12uV	- 9uV
10	39uV	- 36uV
30	111uV	- 109uV
100	367uV	- 369uV

==========

Sheet Resistivity = 36.8e-3 ohm/square

Average Sheet Carrier concentration = 8el6 cm-2

Mobility = 1848.9 cm2/V-sec

Sample Type : Zn/GaAs
Impurity Concentration: Unknown
Doping Process: Furnace Diffusion

==========

Magnetic Field = 0.5 Tesla

I(mA)	Vfor	Vfstat	Vrev	Vrstat
1	0.674mV	0.661mV	-0.673mV	-0.670mV
3	2.021mV	1.995mV	-2.021mV	-2.003mV
10	6.729mV	6.652mV	-6.739mV	-6.669mV
30	20.169mV	19.946mV	-20.206mV	-19.988mV
100	0.067V	0.066V	-0.067V	-0.066V

==========

Magnetic Field=- 0.5 Tesla

I(mA)	Vfor	Vfstat	Vrev	Vrstat
1	0.658mV	0.661mV	-0.66mV	-0.670mV
3	1.975mV	1.995mV	-1.977mV	-2.003mV
10	6.578mV	6.652mV	-6.591mV	-6.669mV
30	19.720mV	19.946mV	-19.758mV	-19.988mV
100	0.065V	0.066V	-0.0661V	-0.0669V

==========

Sheet Resistivity = 1.001 ohm/square

Average Sheet Carrier concentration = 4.19e16 cm-2
(8.38e17 cm-3)

Mobility = 149.01 cm2/V-sec

Sample Type : Se/GaAs
Impurity Concentration: 2.2el2 cm-2
Doping Process: Ion-implantation
Laser anneal intensity: 0.27 Jcm^{-2}

==========

Magnetic Field = 0.5 Tesla

I(uA)	Vfor	Vfstat	Vrev	Vrstat
1	2.79mV	2.68mV	-2.78mV	-2.66mV
3	8.36mV	8.03mV	-8.37mV	-8.01mV
10	27.89mV	26.7mV	-27.88mV	-26.69mV
30	83.8mV	80.2mV	-83.7mV	-80.1mV

==========

Magnetic Field=- 0.5 Tesla

I(uA)	Vfor	Vfstat	Vrev	Vrstat
1	2.8mV	2.68mV	-2.8mV	-2.66mV
3	8.3mV	8.03mV	-8.3mV	-8.01mV
10	27.7mV	26.7mV	-27.7mV	-26.69mV
30	83.1mV	80.2mV	-83.1mV	-80.1mV

==========

Sheet Resistivity = 20554 ohm/square

Average Sheet Carrier concentration = 2.604el2 cm-2

% Carrier Activation = > 100 %

Mobility = 116.5 cm2/V-sec

Sample Type : Se/GaAs
Impurity Concentration: 2.2el2 cm-2
Doping Process: Ion-implantation
Laser anneal intensity: 0.3 Jcm^{-2}

==========

Magnetic Field = 0.5 Tesla

I(uA)	Vfor	Vfstat	Vrev	Vrstat
1	1.7mV	1.7mV	-1.7mV	-1.6mV
3	5.2mV	5.1mV	-5.2mV	-5.0mV
10	17.1mV	17.0mV	-17.1mV	-16.5mV
30	51.3mV	51.0mV	-51.3mV	-49.1mV
100	0.17V	0.169V	-0.17V	-0.164V

==========

Magnetic Field=- 0.5 Tesla

I(uA)	Vfor	Vfstat	Vrev	Vrstat
1	1.7mV	1.7mV	-1.7mV	-1.6mV
3	5.2mV	5.1mV	-5.2mV	-5.0mV
10	17.1mV	17.0mV	-17.1mV	-16.5mV
30	51.6mV	51.0mV	-51.6mV	-51.0mV
100	0.17V	0.169V	-0.171mV	-0.164mV

==========

Sheet Resistivity = 7024 ohm/square

Average Sheet
Carrier concentration = 2.03el3 cm-2

% Carrier Activation = > 100 %

Mobility = 41.47 cm2/V-sec

Sample Type : Se/GaAs
Impurity Concentration: 2.2el2 cm-2
Doping Process: Ion-implantation
Laser anneal intensity: 0.33 Jcm^{-2}

==========

Magnetic Field = 0.5 Tesla

I(uA)	Vfor	Vfstat	Vrev	Vrstat
1	2.185mV	2.13mV	-2.243mV	-2.23mV

==========

Magnetic Field= 0.6 Tesla

I(uA)	Vfor	Vfstat	Vrev	Vrstat
1	2.181mV	2.13mV	2.258mV	2.23mV

==========

Sheet Resistivity = 5788 ohm/square

Average Sheet
carrier concentration = 1.48el3 cm-2

% Carrier Activation = > 100 %

Mobility = 69.07 cm2/V-sec

Sample Type : Si/GaAs
Impurity Concentration: 6e13 cm-2
Doping Process: Ion-implantation
Laser anneal intensity: 0.23 Jcm^{-2}

==========

Magnetic Field = 0.5 Tesla

I(uA)	Vfor	Vfstat	Vrev	Vrstat
1	36.51mV	36.16mV	-36.57mV	-36.22mV
3	0.109V	0.108V	-0.109V	-0.108V
10	0.366V	0.362V	-0.366V	-0.363V
30	1.098V	1.087V	-1.100V	-1.089V

==========

Magnetic Field=- 0.5 Tesla

I(uA)	Vfor	Vfstat	Vrev	Vrstat
1	37.26mV	36.97mV	-37.32mV	-37.0mV
3	0.112V	0.111V	-0.112V	-0.111V
10	0.373V	0.371V	-0.373V	-0.371V
30	1.123V	1.115V	-1.123V	-1.115V

==========

Sheet Resistivity = 108268 ohm/square

Average Sheet
Carrier concentration = 1.02e12 cm-2

% Carrier Activation = 1.7 %

Mobility = 56.59 cm2/V-sec

Sample Type : Si/GaAs
Impurity Concentration: 6e13 cm-2
Doping Process: Ion-implantation
Laser anneal intensity: 0.24 Jcm^{-2}

==========

Magnetic Field = 0.5 Tesla

I(uA)	Vfor	Vfstat	Vrev	Vrstat
1	3.233mV	3.160mV	-3.200mV	-3.160mV
3	9.701mV	9.510mV	-9.660mV	-9.530mV
10	32.18mV	31.80mV	-32.2mV	-31.01mV
30	95.30mV	94.2mV	-96.3mV	-95.40mV

==========

Sheet Resistivity = 179158 ohm/square

Average Sheet
Carrier concentration = 6.745e12 cm-2

% Carrier Activation = 11 %

Mobility = 5.1 cm2/V-sec

Sample Type : Si/GaAs
Impurity Concentration: 6e13 cm-2
Doping Process: Ion-implantation
Laser anneal intensity: 0.29 Jcm^{-2}

Magnetic Field = 0.5 Tesla

I(uA)	Vfor	Vfstat	Vrev	Vrstat
1	4.476mV	4.510mV	-4.481mV	-4.550mV
3	13.44mV	13.57mV	-13.456mV	-13.58mV
10	44.76mV	45.52mV	-44.71mV	-45.14mV
30	0.134V	0.135V	-0.134mV	-0.135mV
100	0.444V	0.447V	-0.439V	-0.443V
300	1.311V	1.320V	-1.278V	-1.288V

Sheet Resistivity = 8594.5 ohm/square

Average Sheet
Carrier concentration = 7.848e12 cm-2

% Carrier Activation = 13.08 %

Mobility = 92.66 cm2/V-sec

Sample Type : Si/GaAs
Impurity Concentration: 6e13 cm-2
Doping Process: Ion-implantation
Laser anneal intensity: 0.32 Jcm^{-2}

==========

Magnetic Field = 0.5 Tesla

I(uA)	Vfor	Vfstat	Vrev	Vrstat
1	1.71mV	1.74mV	-1.65mV	-1.71mV
3	5.10mV	5.16mV	-5.01mV	-5.11mV
10	16.8mV	17.13mV	-16.7mV	-17.13mV
30	50.1mV	51.2mV	-50.5mV	-51.5mV
100	0.166V	0.169V	-0.168V	-0.172V
300	0.509V	0.520V	-0.542V	-0.556V

==========

Sheet Resistivity = 27420 ohm/square

Average Sheet
Carrier concentration = 8.89e12 cm-2

% Carrier Activation = 14.8 %

Mobility = 25.63 cm2/V-sec

Sample Type : Si/GaAs
Impurity Concentration: 2el4 cm-2
Doping Process: Ion-implantation
Laser anneal intensity: 0.24 Jcm^{-2}

==========

Magnetic Field = 0.5 Tesla

I(uA)	Vfor	Vfstat	Vrev	Vrstat
1	-6uV	3uV	3uV	-6uV
3	-17uV	7uV	12uV	-10uV
10	-51uV	24uV	48uV	-26uV
30	-151uV	73uV	150uV	-72uV
100	-505uV	230uV	504uV	-250uV

==========

Magnetic Field = -0.5 Tesla

I(uA)	Vfor	Vfstat	Vrev	Vrstat
1	9uV	2uV	-13uV	-4uV
3	33uV	8uV	-37uV	-10uV
10	110uV	26uV	-125uV	-30uV
30	340uV	83uV	-322uV	-87uV
100	1.107mV	0.289mV	-1.07mV	-0.283mV

==========

Sheet Resistivity = 693.7 ohm/square

Average Sheet Carrier concentration = 3.85el3 cm-2

% Carrier Activation = 19.25 %

Mobility = 234 cm2/V-sec

Sample Type : Si/GaAs
Impurity Concentration: 2e14 cm-2
Doping Process: Ion-implantation
Laser anneal intensity: 0.265 Jcm^{-2}

==========

Magnetic Field = 0.5 Tesla

I(uA)	Vfor	Vfstat	Vrev	Vrstat
1	30uV	34uV	-31uV	-36uV
3	93uV	105uV	-93uV	-107uV
10	309uV	352uV	-309uV	-352uV
30	0.982mV	1.058mV	-0.929mV	1.058mV
100	3.093mV	3.524mV	-3.094mV	-3.523mV

==========

Magnetic Field = -0.5 Tesla

I(uA)	Vfor	Vfstat	Vrev	Vrstat
1	39uV	35uV	-40uV	-36uV
3	118uV	106uV	-120uV	-107uV
10	397uV	352uV	-395uV	-353uV
30	1.188mV	1.06mV	-1.189mV	-1.061mV
100	3.959mV	3.532mV	-3.960mV	-3.532mV

==========

Sheet Resistivity = 309.1 ohm/square

Average Sheet Carrier concentration = 7.4e13 cm-2

% Carrier Activation = 37 %

Mobility = 273.2 cm2/V-sec

Appendix II

Procedures for Hall effect measurements

The following section outlines the steps taken to prepare the pulsed laser annealed samples for the Hall measurements. As mentioned earlier, the samples investigated in this project were all encapsulated. Since it is imperative for the samples to have good ohmic contacts across the active region, it is necessary for all traces of the encapsulants to be removed from the active region. To provide a good metal/semiconductor interface, indium a group III metal was chosen. The reason for this choice is that indium posesses a low melting temperature hence enabling the contact wires to be soldered onto the metal with greater ease, as described in section 2.2. This will become apparent as the steps to this procedurial section are explained.

[1] Rinse sample in concentrated HF acid according to etch rate of encapsulants. This removes all traces of Si_3N_4 on active region of sample. **CAUTION: Do not over-etch as HF acid may remove active region as well. Thus, always refer to wafer specifications for removing encapsulants**

[2] Rinse sample in deionised water for 3 minutes. Remove and blow dry sample.

[3] Cut 4 small pieces of indium, each large enough to cover the "ears" of the clover leaf sample.

Rinse indium pieces in acetone for 3 minutes and follow by immersing the pieces in deionised water for 3 minutes.

[4] Place indium contacts carefully on each "ear" of the sample.

[5] Since it is desirable to obtained a good ohmic contact across the active region, it is necessary to sinter (or diffuse) the indium contacts into the surface of the sample. The sintering process follows by placing the sample from step[4] into a furnace set at a temperature of 380^{o}C in an ambient of hydrogen and nitrogen at a 50:50 ratio for a period of 5 minutes. The ambient gases prevents the contacts from being oxidised.

[6] Remove the sample from the furnace and allow it to cool for 10 minutes.

[7] Mount the sample onto the Hall probe as described in figure 2.3b of section[2.3]. Paraseal wax is suggested for adhesive purposes. Note that the contact wires on the probe are to be soldered onto the indium contacts. This is to be done with great care to avoid the melted indium from overlapping to the other contacts. This is by no means an easy task, hence a steady hand and great patience is a pre-requisite here.

[8] Sample is ready for Hall measurements.

Appendix III

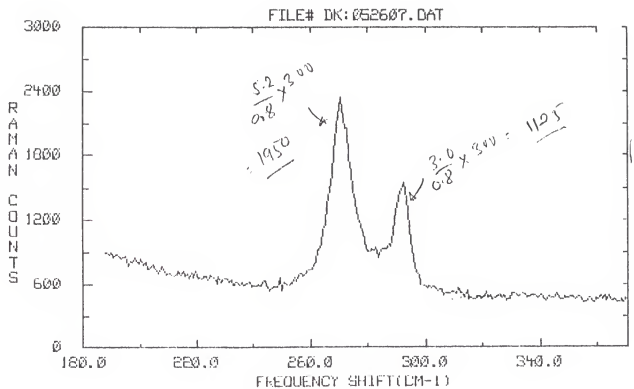
FILE# DK:052607.DAT
RAMAN COUNTS
3000
2400
1800
1200
600
0
180.0
220.0
260.0
300.0
340.0
FREQUENCY SHIFT(CM-1)
5.2/0.8 x 300 = 1950
3.0/0.8 x 300 = 1125

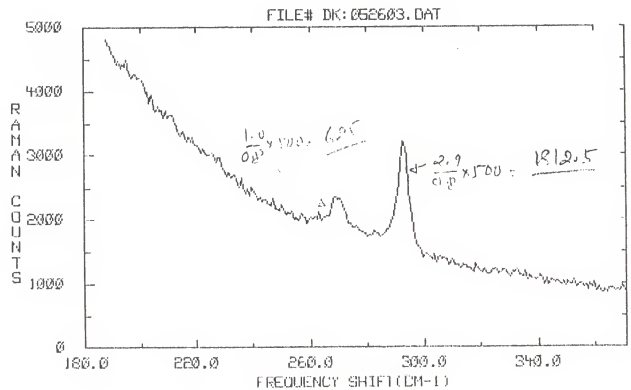
FILE# DK:052603.DAT
5000
4000
3000
2000
1000
0
RAMAN COUNTS
180.0
220.0
260.0
300.0
340.0
FREQUENCY SHIFT(CM-1)
1.0/0.15 x 100 = 667
2.9/0.2 x 1500 = 18120.5

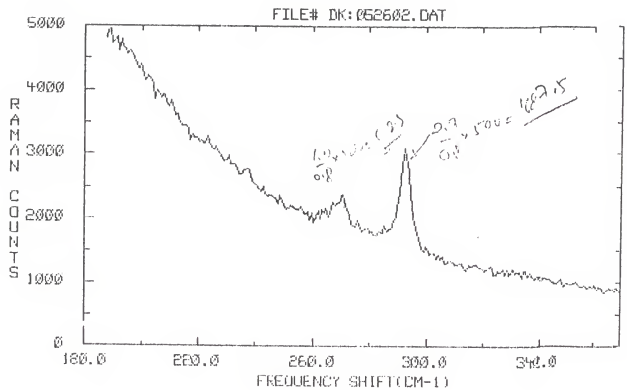
FILE# DK:052602.DAT
5000
4000
3000
2000
1000
0
RAMAN COUNTS
180.0
220.0
260.0
300.0
340.0
FREQUENCY SHIFT(CM-1)

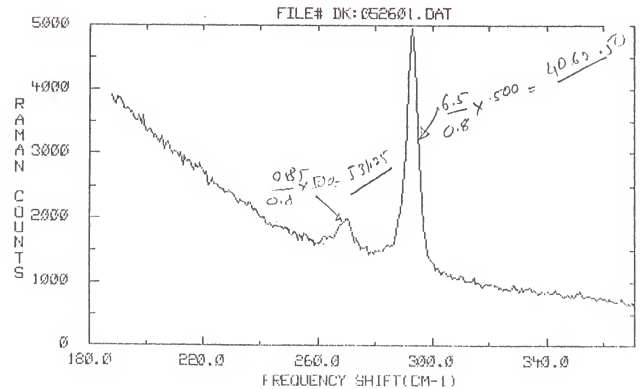
FILE# DK:052601.DAT
5000
4000
3000
2000
1000
0
RAMAN COUNTS
180.0
220.0
260.0
300.0
340.0
FREQUENCY SHIFT(CM-1)
0.8/0.8 x 500 = 500
6.5/0.8 x 500 = 4062.5

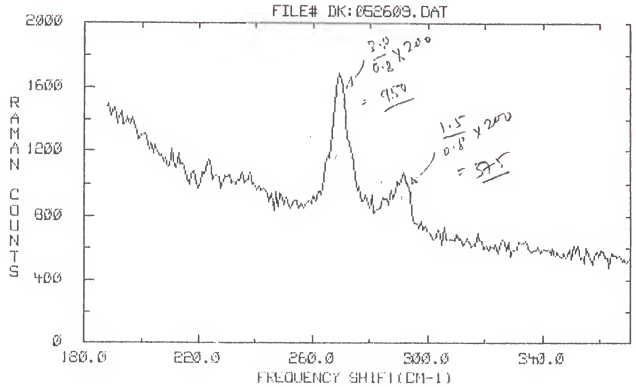
FILE# DK:052609.DAT
2000
1600
1200
800
400
0
RAMAN COUNTS
180.0
220.0
260.0
300.0
340.0
FREQUENCY SHIFT(CM-1)
3.9/0.2 x 200
= 975
1.5/0.8 x 200
= 375

Appendix IV

Determining energy intensity of beam spot

The conversion factor for the laser beam intensity in section 2.0 was estimated for a 3 by 2 mm aperture. However, the following procedures for determining power intensity is applicable to apertures of all sizes.

[1] First measure maximum voltage transmitted using a calorimeter across the aperture. Remove all light filters. As a precaution to prevent the calorimeter from damage, set the pulse rate to 5pulses/sec.

[2] Assuming laser power set at 100mJ:

* Note: 100mV ---------- 1W
as calibrated by Scientek Inc. calorimeter model 3600.

24.14mV(Measured across aperture) = 100mJ

Hence,

1mV ---------- 100mJ/24.14= 4.14mJ

Thus, Energy per cm^{-2}:

$4.14mJ/(0.3 \times 0.2)cm^2 = 0.069\ Jcm^{-2}$

Therefore,

1mv ---------- $0.069\ Jcm^{-2}$

Using this conversion factor as a yardstick to our measurements, the maximum laser intensity obtainable would be $1.66\ Jcm^{-2}$. Hence, by using a series of light filters, we were then able to provide a range of intensities for our pulse laser annealing experiments.

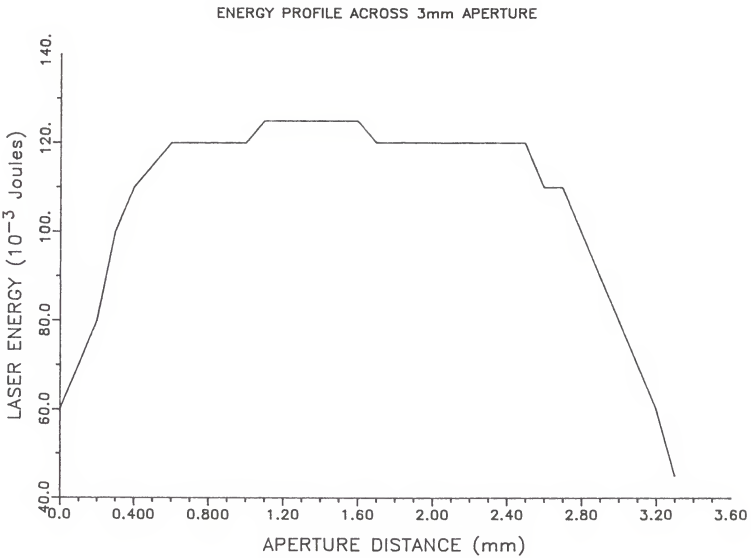
ENERGY PROFILE ACROSS 3mm APERTURE
LASER ENERGY (10^{-3} Joules)
140.
120.
100.
80.0
60.0
40.0
0.0
0.400
0.800
1.20
1.60
2.00
2.40
2.80
3.20
3.60
APERTURE DISTANCE (mm)

Appendix V

Error Analysis

Procedure

A qualitative analysis was performed on the samples to determine a basis for the degree of error estimated in the Hall measurements.

Result

Sample type: Si/GaAs
Dose: $6 \times 10^{13} cm^{-2}$

Equipment	Parameter measured	% error
VARIAN 4 inch Electromagnet System	Magnetic Field (B) in kiloGauss.	+/- 0.23 %
Constant Current source, Model 110	Deviation of current sourced.	+/- 0.1 %
Digital Volt Meter Fluke 8520A	Deviation of Hall potential(V_h)	+/- 1.349 %
DVM Fluke 8520A	Deviation of static potential(in the absense of a magnetic field)	+/- 0.85 %

Conclusion

A significant degree of error was noted for the measurement of the Hall potentials. The voltage reading began fluctuating about 30 seconds after an initial stable reading, largely due to resistive heating across the indium ohmic contacts. The solution to this problem was to take the readings before this effect takes place. To reduce the error involved, the averaged reading for the Hall voltage obtained

for both the forward and reversed directions of the current was used.

Another source of error originated from the static potential readings across the sample i.e voltage readings in the absense of a magnetic field. The +/- 0.85 % error was due to the irradiative effect from the surrounding light source. Hence, we tried to reduce this error by performing these initial potential readings in the dark. As described in the **Experiment** section, the static potentials are then subtracted from the Hall potentials with the result used to calculate its corresponding free sheet carrier concentration.

The error from the Electromagnet system and the Constant current source, on the whole, was almost negligible.

REFERENCES

[1] Shunji Nojima, "Laser annealing effects on ion-implanted GaAs," American Institute of Physics. July, 1982.

[2] L.E. Larson et al, "GaAs High Speed Digital IC technology: An Overview," COMPUTER. October, 1986.

[3] T. W. Sigmon, "UV LASER PROCESSING OF SEMICONDUCTOR DEVICES," Stanford Electronics Laboratories, Stanford,CA 94305.

[4] T.E Haynes et al, "Effectivenes of thin film encapsulants for reducing evaporation during thermal processing of GaAs," Sandia National Labs, Albuquerque,NM 87185.

[5] R.T. Young et al,"Semiconductor Processing with Excimer Lasers," Solid State Technology. November, 1983.

[6] Thomas A. Znotins, "Excimer lasers: An emerging technology in semiconductor processing". Solid State Technology. September, 1986.

[7] A. Compaan et al, "Excimer and Dye laser annealing of silicon nitride capped, Si implanted GaAs Applied Physics Letters, 1986.

[8] A. M. Horak, "Pulsed Laser Annealing of GaAs "A Master's thesis, Kansas State University. 1986

[9] A. Bhat, "Time resolved reflectivity study of pulsed laser irradiated silicon nitride capped GaAs," A Master's thesis, Kansas State University. 1987.

[10] L. J. Van Der Pauw, "A method of measuring the resistivity and Hall coefficient on lamellae of arbitrary shape," Philips technical review. January, 1958.

[11] S. M. Sze, "Semiconductor Devices, Physics and Technology," Wiley Interscience.

[12] Ghandi, "VLSI fabrication principles," Wiley-Inter science.

[13] W.R. Runyan, " Semiconductor measurements and

Instrumentation," Texas Instruments.

[14] H. A. Szymanski, Raman Spectroscopy - Theory and Practice. Plener Press, 1967.

[15] D.V. Lang, "Deep-level transient spectroscopy: A new method to characterise traps in semiconductors," Journal of Applied Physics. July, 1974.

A STUDY OF HALL-EFFECT MEASUREMENT TECHNIQUES ON PULSED LASER ANNEALED GALLIUM ARSENIDE

by

TIMOTHY W.H. CHIN

B.S., Kansas State University, 1985

AN ABSTRACT OF A MASTER'S THESIS

submitted in partial fulfillment of the

requirements for the degree

MASTER OF SCIENCE

Department of Electrical and Computer Engineering

KANSAS STATE UNIVERSITY
Manhattan, Kansas

1988

ABSTRACT

A fully operational pulsed laser annealing system (PLA) using a rare halide Excimer laser (λ=308nm) is described extensively in this thesis. The effectiveness of the system is evaluated by studying the electrical activity of the ion-implanted GaAs samples that have been pulsed laser annealed over a duration of 10 nsecs. Both low dosed as well as very heavily dosed samples were characterized and studied using a conventional Hall effect technique. Among some of the observations in this thesis, our results show that contrary to earlier reports on this topic, a considerable degree of carrier activation was found among the lower dosed samples. To support this, we were able to correlate the results from a light scattering technique (Raman Back-Scattering) that was performed on the same samples to those obtained earlier from the Hall effect measurement technique. As the sample substrates used in this thesis were all capped with a 70 nm layer of silicon nitride, the effects of encapsulants on the carrier activity of the samples during the process of pulsed laser annealing will also be investigated.